LUND UNIVERSITY
Faculty of Science

Review of astrophysical probes of dark matter

Gabriella Szabó

Thesis submitted for the degree of Bachelor of Science

Project duration: 6 months
Examination: Spring 2021

Supervised by Marco Cirelli and Caterina Doglioni

Department of Physics
Division of Particle Physics
May, 2021

Abstract

Research on dark matter has been ongoing for almost a century. Findings show that dark matter makes up 27% of the universe's density and thus it is a crucial component of understanding how the universe came about. This thesis describes the key pieces of evidence for the existence of dark matter and its properties. An emphasis is put on the effects of dark matter on processes in the early universe. Methods of dark matter detection are introduced with a focus on indirect detection experiments. Furthermore, an analysis of positron data measured by the AMS detector from 2011 to 2017 in terms of dark matter is presented.

Contents

List of Abbreviations

SM = Standard Model
DM = Dark Matter
iDMEu = Initiative for Dark Matter in Europe and beyond: Towards facilitating communication and result sharing in the Dark Matter community
CMBR = Cosmic Microwave Background Radiation
CDM = Cold Dark Matter
HDM = Hot Dark Matter
WIMP = Weakly Interacting Massive Particle
LHC = Large Hadron Collider
IACT = Imaging Atmospheric Cherenkov Telescope
AMS-02 = Alpha Magnetic Spectrometer-02
PAMELA = Payload for Antimatter Matter Exploration and Light-nuclei Astrophysics

Chapter 1

Introduction

The Standard Model (SM) of particle physics is a well understood model that extensively describes the nature of ordinary matter. However, the particles that comprise the SM only account for 20 % of the universe's total matter [1]. The rest is dark matter (DM). Even though there is evidence that DM constitutes such a large portion of matter, little is known about it. Research to understand the nature of dark matter has been ongoing since the 1930s [2], and since then it has been approached from many different angles. For this reason, the dark matter research community comprises theorists and experimentalists across a wide variety of fields who work, among others, on direct, indirect and collider experiments. Direct detection searches investigate direct interactions of DM with ordinary matter on Earth, indirect detection experiments search for products of DM interactions coming from space, and collider experiments attempt to produce DM particles through collisions of SM particles. Discovering the nature of dark matter would answer existing questions about the composition and structure of our universe. It would also potentially facilitate the development of new physics beyond the Standard Model, as evidence indicates to the exotic nature of DM [2].

This project is a collaborative work within the *Initiative for Dark Matter in Europe and beyond: Towards facilitating communication and result sharing in the Dark Matter community* (iDMEu). The objective of the initiative is to create a new platform which cultivates a collaborative spirit through result sharing, with the goal of advancing dark matter research.

There are three primary goals of the project: 1.To review evidence of DM and the DM properties it points to. 2. To review indirect detection of DM and create a table of current and developing DM indirect detection experiments for the iDMEu website. 3. To perform an analysis of results from indirect searches through the analysis of positron data from the Alpha Magnetic Spectrometer (AMS-02) [3] in terms of dark matter.

In Chapter 2 a summary of the most compelling DM evidence is presented, as well as the known and theorized characteristics of DM and how they tie into the formation of the universe. Chapter 3 introduces indirect detection and its three main experimental categories: gamma ray experiments, cosmic ray experiments, and neutrino experiments. A sample of the table created for the iDMEu website is also provided. Chapter 4 describes

the work that was done on theoretical predictions of DM, such as production of positrons from DM annihilation, and the propagation of the generated positrons. The data was then used to interpret experimental positron flux data from one of the indirect detection experiments included in the review table, the AMS-02 detector.

Chapter 2

Theoretical Background

2.1 Early observations

The first speculations on the existence of non visible matter came about in the 1930s when scientists were attempting to estimate the mass of galaxy clusters using their velocity dispersion [4]. Comparing the total mass of these structures to the amount of luminous matter revealed a high mass-to-light ratio for some galaxies and clusters. This data implied the presence of large amounts of non-luminous, dark matter in the universe. In spite of these surprising results the topic of dark matter did not become a pressing issue until much later.

In the 70s, with the development of techniques useful to measure galactic rotation curves, physicists were able to better identify the presence and determine the location of this non-radiating matter. Advancements in radio technology, namely the detection of the 21-centimeter line which penetrated interstellar dust, led to the optical observation of the structure of galaxies [2]. This allowed physicists to construct rotation curves, plots of the orbital velocity of matter in a galaxy as a function of the distance from its centre [5]. Following Newtonian gravity, the velocity was expected to decrease outside the galactic disc. Instead, the rotation curves displayed a flattening. The result implied the existence of dark matter at large galactocentric distances.

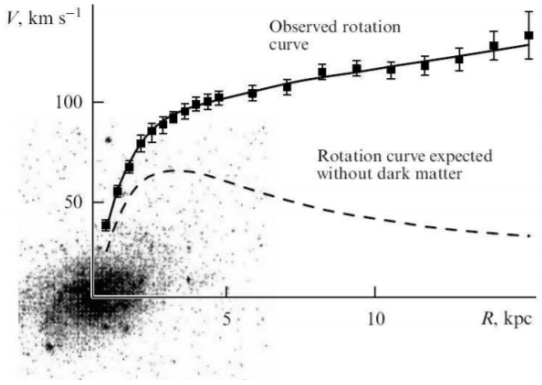

Figure 2.1: Rotation curve of the M33 galaxy [6]

Another piece of evidence for the presence of DM came about in 2004 when physicists observed the remnants of the collision of two galaxy clusters, known as the Bullet Cluster (Figure 2.2). During this event the clusters passed through each other, however their gas clouds collided. The temperature increased which resulted in the emission of X-rays, and the gas traveled further with decreased velocity [7]. Gravitational lensing, a phenomenon in which light is deflected by a massive object that acts as a lens due to its gravitational potential [8], was used to probe the mass of the system. The combined gravitational lensing and X-ray measurements showed that the mass was concentrated at the sides of the galaxies instead of the intra-cluster matter [9]. This result indicated that the clusters contained a high density of DM. Furthermore, as the clusters passed through each other, the DM traveled on uninterrupted unlike normal matter.

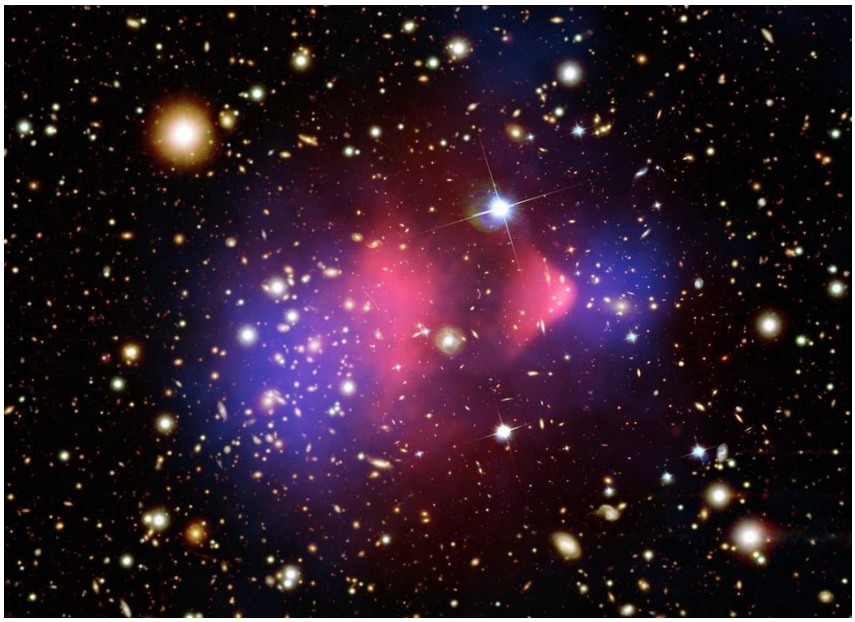

Figure 2.2: Image of the Bullet Cluster with overlaid X-ray emission data (pink) and gravitational lensing data (blue) [9]

As a result of these observation it was concluded that DM is neutral in terms of the electromagnetic force; it does not emit or absorb electromagnetic radiation. Furthermore, as it has not been observed so far, it does not interact strongly with ordinary matter. Thus, DM does not dissipate energy and does not collapse to a disc like galaxies made up of ordinary matter do. Instead, it is enclosed in a DM halo around the galaxy. The distribution of DM within the galaxy halo can be described using various DM density profiles, which have been identified through simulations of DM particles [2].

2.2 Structure formation

Another discovery that greatly improved our understanding of DM is the Cosmic Microwave Background Radiation (CMBR). CMBR is relic radiation which provides a picture of the composition of the early universe. Through CMBR, physicists were able to

determine the amount of dark matter in the universe as well as gain a better understanding of structure formation in the early universe [10].

At the time of the Big Bang the universe was very hot and dense. Within a fraction of a second the inflationary phase began, during which the universe rapidly expanded and cooled. The accelerated expansion led to energy density variations to be stretched out, later resulting in the homogeneity of the universe at large scales. However, there were still slight variations in the inflation field due to quantum fluctuations [11].

After inflation the universe became radiation dominated [11], meaning its total energy density, and as a consequence its evolution, was dominated by species behaving like radiation, such as photons or relativistic particles. Primordial nucleosynthesis took place, and through fusion, light nuclei like deuterium and lithium were formed. However, the electrons were free and unable to bond due to to the extreme heat and radiation; the universe was ionized and opaque. At 380 000 years the universe became cool enough for electrons to be captured, creating stable neutral atoms. This point in the timeline of the universe is called recombination. Light was able to escape and propagate freely and those photons, redshifted, are now detected as CMBR (Figure 2.3) [12].

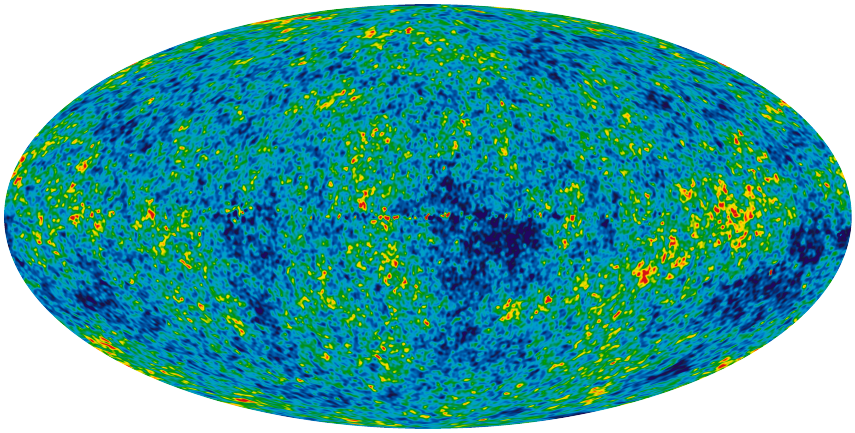

Figure 2.3: Image of Cosmic Microwave Background

The anisotropies that can be seen in the CMBR are the result of the quantum fluctuations in the inflation field expanding, creating regions of over- and underdensity [13]. The higher density regions had higher gravitational potential and attracted matter. For ordinary matter, radiation pressure counteracted the attraction, resulting in the oscillation of the perturbations. However, DM was only affected by the gravitational force which led to its capture in potential wells and subsequent collapse into DM halos. Within the halos ordinary matter dissipated energy and became gravitationally bound forming stars and consequently galaxies [14].

Physicists performed N-body simulations reproducing the dynamics of the early universe and it was found that the velocity of DM particles at the time of matter domination affected structure formation. If DM particles were relativistic in this phase, structure formation would have occurred in a top-down sequence; large halos would have appeared first and later broke up into smaller halos. Relativistic DM is also known as hot dark

matter (HDM). In the case of non-relativistic DM particles, or cold dark matter (CDM), smaller halos would have been first to form, followed by mergers into larger halos [2]. Comparisons of the results of such simulations to observations of halos showed that CDM is the more likely DM candidate.

2.3 WIMPs as DM candidates

A good DM candidate must be produced in the early universe in the right amount, i.e. the one that corresponds to the DM cosmological density today as determined by cosmological measurements. A popular class of candidates of CDM that fits this requirement is that of Weakly Interacting Massive Particles (WIMPs). WIMPs are weakly interacting particles with a mass range of approximately 10 GeV to 100 TeV [15].

More precisely, the theory is that DM particles are thermal relics, meaning they interacted with ordinary particles in the early universe. After the Big Bang matter was in thermal equilibrium; the annihilation and production rate of DM particles were equal. As the universe expanded, the temperature cooled and the amount of available energy decreased. When the temperature dipped below the mass of DM particles, production stopped. Annihilation continued until the expansion rate exceeded the interaction rate. This moment in time is called the "freeze out" of the particle[16].

Following freeze out, the DM abundance remains constant. The higher the annihilation cross section of the particle, the higher is the probability of interaction, and thus the smaller is the abundance [17]. The annihilation cross section of WIMPs directly gives the right DM abundance, and this is also called the 'WIMP miracle'.

2.4 Searches for DM

DM searches are conducted using different methods, and each experiment generally targets the main characteristics of a certain DM candidate. The three main experimental methods that look for DM with WIMP energy ranges are direct detection, collider experiments and indirect detection. This section gives a brief introduction to direct detection and collider experiments. The method of indirect detection will be described more extensively in the following chapter.

2.4.1 Direct Detection of DM

Direct detection detectors are located deep underground and attempt to measure the recoil energy of a nucleus hit by a dark matter particle. It is assumed that, while most dark matter particles stream through Earth without any effects, some will interact with the detector target a few times a year. When this happens, the affected nucleus will emit energy in the form of scintillation or phonons at the scale of a few keVs [10]. In order to be able to detect such small signals the sensitive apparatuses have to be shielded from much more frequent cosmic rays, and thus are placed underground. A series of improved

direct detection experiments are in development which will have higher sensitivities and will be able to measure a more extended range of masses and scattering cross-sections.

2.4.2 Collider Experiments

Dark matter particles with masses around the TeV could be produced from high-energy collisions of ordinary matter, like the ones that occur at the Large Hadron Collider, a proton-proton collider at CERN. Such an event would be detected as a large amount of transverse momentum that cannot be accounted for, as it would escape detection. Another method, to look for signs of certain models of dark matter, is looking for the particles that mediate the interaction between ordinary matter and dark matter, which can also decay to Standard Model particles. There are different mediator candidates in different models of DM production at colliders. Examples of mediator particles are the Z boson, Higgs boson, or for light dark matter models a new dark boson (often called dark photon, or Z') with a spin 1 and a non-zero mass [18].

Chapter 3

Indirect Detection of DM

The focus of this project is indirect detection experiments. Indirect detection experiments search for the products of DM particle annihilations. In most theories, DM particles are predicted to annihilate in pairs when they meet . In many DM models, it is assumed that there exist two equal populations of DM particles and antiparticles in the Milky Way Galaxy and in the universe at large. The process of annihilation is rare and it does not deplete at all the DM content of a galaxy or the universe, however it is frequent enough that some signals can be detected [19]. The annihilation process is the same as it was in the early universe before the "freeze-out", however it happens in a much more rarefied environment, meaning less interactions occur. Some theories suggest that DM particles can also decay [19]. DM decay is also an extremely rare event and does not affect the overall DM density. Dark matter can directly annihilate to high energy gamma rays or to unstable particles that subsequently decay to stable particles. Indirect detection experiments look for these signals. The three main categories of indirect detection experiments are gamma ray experiments, charged cosmic ray experiments and neutrino experiments. At the end of the chapter a sample of the table made for the future iDMEu website, with examples for each category of experiments can be found.

3.1 Gamma Ray Experiments

A great advantage of gamma-ray experiments is that gamma-rays do not lose much intensity as they travel through space, and they are not affected by magnetic fields, thus the detected signals are undisturbed by astrophysical effects [20]. Gamma rays move along a straight line and point back to their source, which is a region where DM is densest.

DM annihilations/decays can produce different gamma-ray spectra. A direct DM annihilation to gamma radiation would produce a spike of energy in the detector corresponding to the mass of DM, as all DM energy is transferred to the photons. DM annihilation to other ordinary particles generates gamma signals through the decay of these particles. Such events produce more broad energy signals. These cases are examples of prompt gamma ray emission from DM, as the radiation is produced at the moment of the annihilation or shortly after. As a result, one way of classifying detectors is by their capability to detect high or low energy radiation. Another important characteristic of detectors is their location. There are ground based and space based gamma ray telescopes. The methods

used for detection are different due to the difference in the medium that detection occurs in.

3.1.1 Targets

An important question in indirect detection is where to direct the telescopes. The highest rate of DM annihilations is most likely to occur in areas of high DM density. A large volume for detection and relatively short distance to Earth are also important factors as they affect the flux of the particles. Lastly, it is essential to consider background radiation that could interfere with the detection signal. A good target should have low background or the background should come from well understood sources [20].

A common target is the center of the Milky Way. It is the nearest and brightest predicted dark matter annihilation target. The Fermi Gamma-Ray Space Telescope has detected an excess of potential gamma rays at the Galactic Centre that points to DM. However, the density distribution of DM close to the Galactic Center is not well understood. The source could be a collection of unresolved pulsars or other undetected ordinary astrophysical phenomena, so the result is not definitively attributed to DM [21].

Another significant target is dwarf spheroidal galaxies. Even though they are further away, dwarf galaxies contain a high density of DM with low gamma ray backgrounds making them a good, clear source. Other targets include galaxy clusters and the isotropic gamma-ray background, which should be affected by DM annihilations, both in the Milky Way halo and the rest of the universe [21].

3.1.2 Methods

One method of high energy gamma ray detection is using an Imaging Atmospheric Cherenkov Telescope (IACT). When a high energy gamma ray enters the atmosphere, pair production occurs as nuclei become available near the photon. A cascade of particles, an extensive air shower, is created as the generated electron-positron pair undergoes Bremsstrahlung and further pair-production occurs. Concurrently, as the charged particles traverse the atmosphere with a higher velocity than light moves in the medium, a rapid flash of Cherenkov radiation is emitted [22]. The IACT collects the radiation with an upward facing mirror which focuses the radiation onto an array of photomultiplier tubes. The produced image provides information about the type of the initial particle, its energy and direction [23].

Another method is detecting the air shower directly using an Air Shower Array fitted with scintillators. Air Shower Arrays are advantageous due to a larger field of view. However, their sensitivity is lower and they are worse at differentiating cosmic and gamma ray signals [23]. In Water Cherenkov Detectors, water tanks are used instead of scintillators. In such detectors, the signal is Cherenkov light created from the change of medium from air to water.

3.2 Cosmic Ray Experiments

Models of cosmic ray productions in the Milky Way Galaxy are fairly accurate, with predictions agreeing with observations. This makes cosmic ray experiments a useful tool of DM searches as background processes are rather well understood. The cosmic rays produced in the universe are predominantly comprised of matter over antimatter [20]. As mentioned above, in most theories DM annihilation and decay occurs in a way that produces an equal amount of particles and antiparticles. Therefore, in the case of DM annihilation or decay to cosmic rays, an excess of antimatter charged particles should be produced compared to the predicted cosmic-ray spectrum. Consequently, indirect detection experiments mainly search for excesses on top of the fluxes of otherwise under-abundant antiparticles, such as positrons, antiprotons, and antideuterons [20].

A disadvantage of cosmic ray searches is that charged particles are affected by magnetic fields, collisions and astrophysical events during their propagation. Unlike gamma rays, the location of the source and exact initial energy of the cosmic rays are unknown upon detection as the particles travel randomly and are subjected to energy losses. A more extensive description of cosmic ray production, propagation and its effects is provided in the project section of the thesis.

3.2.1 Method

The three types of cosmic ray detectors are ground based, satellite based and balloon-borne experiments. However, not all experiments are useful for DM detection as many look for cosmic rays that are too energetic to be a DM signal. The most useful DM cosmic ray detectors are space based as they are able to measure cosmic rays of a wide energy range. These experiments use similar equipment for detection. The main components of the detectors are an anti-coincidence detector, which rejects unwanted particles, a tracker with a magnet, which measures the momentum of the particles and their charge, and a calorimeter, which measures the energy [24] [25] . Not all detectors have a magnet, which means these detectors cannot distinguish between a particle and an antiparticle signal. This is a disadvantage for DM searches, since as explained above DM indirect detection is easier with antiparticles.

3.3 Neutrino Experiments

Neutrinos are difficult to detect due to their low interaction cross section. However, for the same reason neutrinos are able to pass through large amounts of matter without interacting with it . Some models suggest that DM gets captured and accumulates in the core of the Sun and Earth [19]. A high enough density of particles leads to annihilations that generate neutrinos. The high energy neutrinos then escape the core without substantial energy losses and can be detected at Earth. Physicists searching for DM neutrino signals have to take into consideration not only the annihilation cross section of DM but also the DM capture rate [20], as it affects the amount of neutrinos produced and thus the detection flux.

3.3.1 Method

All neutrino experiments use the same principal of detection. They are well isolated by being placed underground, under ice or underwater to minimize background signals. An array of photomultipliers detects Cherenkov radiation that is produced by the electrons or muons that are produced when the neutrino interacts with the detecting medium, or the rock surrounding it[26]. The IceCube experiment uses ice as the detecting medium which allows for better resolution [27]. On the other hand, using water makes it easier to suppress background radiation.

3.4 iDMEu Table

A part of the thesis was creating a Microsoft Excel (2021) table of currently operating and future indirect detection experiments for the future iDMEu website. The table will appear on the platform among a variety of other experiments dedicated or connected to DM research. The table will allow for easy access to information about DM experiments. The table below (Figure 3.1) shows a sample of the table, with a few examples from the three categories of indirect DM searches discussed above.

Each experiment has its name, status, energy range, homepage, and technical design report (TDR) listed. In regards to status, all experiments are either ongoing or in development. Indirect detection experiments that have terminated their operation are not included, as the aim of the initiative is the sharing of new results within the dark matter research community. The mass of DM particle is a central component of building DM models, and it determines the energy of the DM annihilation or decay products. Therefore, it is important to list the energies the detectors are sensitive to, so one can easily check which experimental data would be in the energy range of a given DM candidate. The information about the energy of the experiments was found on the homepage of each experiment. It was then verified by looking through recent publications and searching for specifications of performance.

The TDR is a useful document that describes the experiment, details the design and gives a full specification of the detector and its performance. The TDRs were found by searching the name of the experiment on the arXiv, IOPscience, and Inspire HEP websites, and also by looking through the earlier publications listed on the homepage of the experiment. Additional documents were added to experiments that were upgraded or modified their design. For some experiments it was difficult to find the exact TDR, so in these cases articles that resembled the TDR and described the design of the experiment were added.

Gamma ray experiments	Location	Status	Energy range	Homepage	TDR
H.E.S.S. - High Energy Stereoscopic System	The Khomas Highland, Namibia	In operation since summer, 2002	20 GeV - 100 TeV	https://www.mpi-hd.mpg.de/hfm/HESS/	https://arxiv.org/pdf/astro-ph/0308246.pdf
VERITAS - Very Energetic Radiation Imaging Telescope Array System	Fred Lawrence Whipple Observatory, southern Arizona, USA	In operation since February, 2004	50 GeV - 50 TeV	https://veritas.sao.arizona.edu/	https://arxiv.org/pdf/astro-ph/0108478.pdf
MAGIC - Major Atmospheric Gamma Imaging Cherenkov Telescopes	La Palma, Spain	MAGIC-I in operation since October 2004, MAGIC-II in operation since 2009	30 GeV - 100 TeV	https://magic.mpp.mpg.de/	https://magic.mpp.mpg.de/backend/publication/show/133
Charged cosmic ray experiments	**Location**	**Status**	**Energy range**	**Homepage**	**TDR**
CALET - CALorimetric Electron Telescope	Low Earth orbit, part of the International Space Station	In operation since August, 2015	e^+ / e^-: 1 GeV - 20 TeV	http://calet.pi.infn.it/	https://iopscience.iop.org/article/10.3847/1538-4365/aad6a3
DAMPE - DArk Matter Particle Explorer	Low Earth orbit	In operation since December 17, 2015	e^-: 5 GeV- 10 TeV	http://dpnc.unige.ch/dampe/	https://arxiv.org/abs/1706.08453
LHAASO - Large High Altitude Air Shower Observatory	Haizi Mountain, Sichuan Province, China	In operation since April, 2019	cosmic rays: 1 TeV - 1 000 TeV	http://english.ihep.cas.cn/lhaaso/	https://arxiv.org/pdf/1905.02773.pdf
Neutrino experiments	**Location**	**Status**	**Energy range**	**Homepage**	**TDR**
Super-K - Super-Kamiokande	Kamioka mine,Hida city, Gifu Prefecture, Japan	In operation since April 1, 1996	3.5 MeV - a few 100 GeV	http://www-sk.icrr.u-tokyo.ac.jp/sk/index-e.html	https://inspirehep.net/literature/607144
IceCube Neutrino Observatory	Amundsen–Scott South Pole Station , Antarctica	In operation since 2005, completed in December, 2010	100 GeV - 1 EeV	https://icecube.wisc.edu/	https://arxiv.org/abs/1007.1247
ANTARES - Astronomy with a Neutrino Telescope and Abyss environmental RESearch project	Mediterranean Sea, off the coast of Toulon, France	In operation since 2008	20 GeV - 100 TeV	https://antares.in2p3.fr/	https://arxiv.org/abs/1104.1607

Figure 3.1: Sample table of the indirect detection experiments table created for the future iDMEu website

Chapter 4

Project

4.1 Theoretical predictions

As mentioned before the aim of the project was to take existing theoretical predictions of the positron flux produced by DM annihilations, including the e^+ propagation in the Galaxy, and superimpose such predictions with AMS data to determine whether it is possible to explain AMS data in terms of DM and, if yes, which spectrum fits best. All plots and calculations were made using Mathematica [28]. The numerical tools that were needed to plot the predictions from DM models were taken from the "PPPC 4 DM ID: A Poor Particle Physicist Cookbook for Dark Matter Indirect Detection" website [29] .

4.1.1 Positron fluxes at production

First, the positron fluxes at production were plotted using Ref. [30]. The PPPC 4 DM ID website provided the option of 28 primary channels, 7 secondary channels and a DM mass range from 5 GeV to 100 TeV. The mathematical functions from the website, that produced the fluxes, were computed using the Pythia [31] event generator. Electroweak emissions were included in the event generator in order to be able to see the effects of W and Z radiation [29]. The importance of the inclusion of electroweak corrections is further explained when describing the plot of the positron annihilation channel.

Since the aim of the project was to see the fluxes of positrons, the secondary channel was chosen to be positrons. The DM particle mass parameter was set to 1 TeV. The chosen primary channels were the following particles paired with their respective antiparticle: charged leptons e, μ, τ; quarks q, c, b, t, where q is a light quark; bosons W,Z, h, where h is the Higgs boson; and photons γ.

The process that Figure 4.1 represents is the annihilation of two 1 TeV DM particles into the primary particles listed above that further decay and produce a positron flux. The y-axis is the flux or the number of positrons as a function of their energy normalized by the mass of DM. The x-axis is the kinetic energy normalized by the DM mass; the quantity is denoted by x. To better understand the flux of positrons yielded by the DM annihilations, a few of the plots are interpreted qualitatively in the following text.

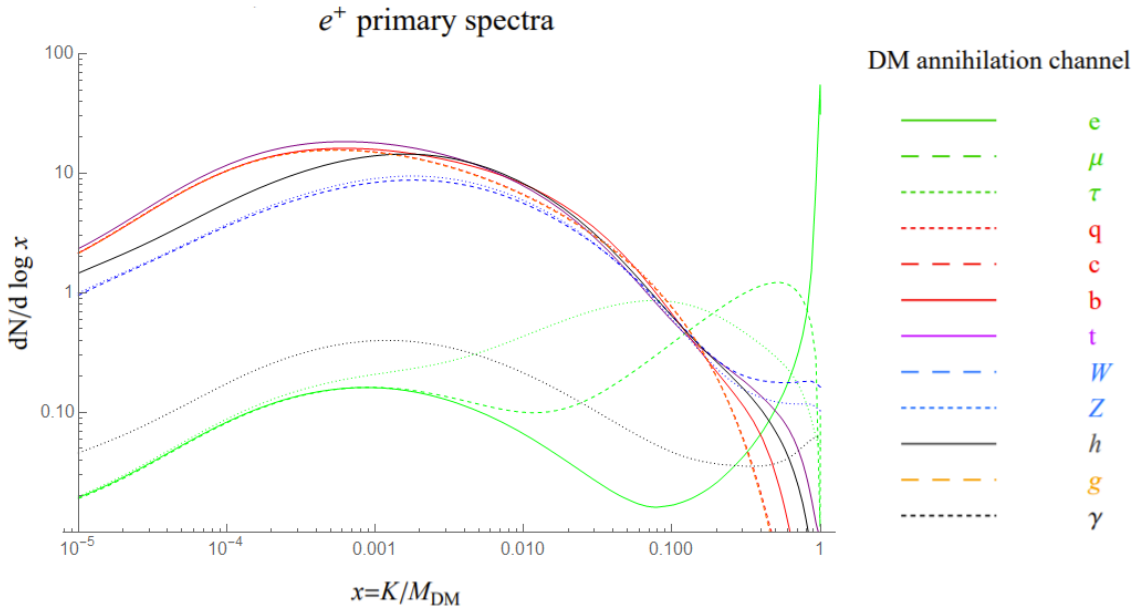

Figure 4.1: Fluxes of positrons produced from annihilation of DM particles into primary particles that further decayed to positrons.

The positron spectrum produced by the DM annihilation through the W annihilation channel is represented by the long dashed blue line. The spectrum has a wide peak at lower energies and it plateaus when the energy is equal to the DM mass at $x = 1$. The spectra is the result of the different possible decay channels.

As the 1 TeV DM particle pair annihilates to the W^+W^- pair, half of the energy is transferred to each boson. 80 GeV of energy is expended on providing the rest mass of each W boson and the rest is available as kinetic energy. The W^+W^- pair then decays. The decay can occur leptonically or hadronically. The leptonic decay has a branching ratio of 11% for each generation [32], meaning that in 11% of cases the W^+ boson decays to a positron and neutrino and the W^- boson decays to an electron and an antineutrino. The decay occurs almost immediately due to the weak boson's short lifetime. Consequently, with the appropriate kinematic configuration, the positron will receive close to 1 TeV of energy, the initial mass of the DM particles, which explains the plateau at $x = 1$.

The hadronic channel has a branching ratio of 67% [32]. In the hadronic decay the production of a quark-antiquark pair occurs, which is followed by hadronization and further decay. This proccess creates a slew of particles, which includes low-energy positrons. The low-energy bump, centered around $\sim 10^{-2.5}$ of the intial energy at disposal, corresponds to the significant amount of these low-energy positrons. The same mechanism explains the spectrums of the other bosons and the quark annihilation channels.

Another interesting spectrum is the e^-e^+ annihilation channel, represented by the solid

green line. The plot has a low flux bump at low energies and a peak at $x = 1$. The peak is a result of the direct annihilation of the DM particles to the electron-positron pair, with a complete energy transfer. However, the distribution is not a delta function; it is smeared towards smaller x. This can be explained by final state radiation. Some particles radiate away energy, which is subtracted from the energy of the e^-e^+ pair. The energy loss transforms the function into a smeared distribution. The bump at low energies is created by electroweak radiation. Due to the high energies of the products, electroweak emission is not suppressed and it is possible for the leptons to emit a weak boson. The boson then decays through the process described before, producing a flux of low energy positrons.

4.1.2 Positron fluxes after propagation

After production positrons that travel through the Milky Way Galaxy are subjected to energy losses through collisions, annihilation and other effects. Spectra collected with detectors at Earth are modified by the propagation. Therefore, in order to be able to identify a potential DM positron signal, it is important to understand the factors that alter the initial flux.

The function that produces the flux after propagation was taken from PPC 4 DM ID [29] [33]. The function encompasses the spectrum at production and a propagation function that incorporates relevant astrophysical effects. The parameters that can be changed are: the primary channel of annihilation, the mass of DM, the DM annihilation cross section, the magnetic field configuration, the DM halo profile, and the propagation parameter. The options for the parameters are listed in Figure 4.2.

primary = eL, eR, e, μL, μR, μ, τL, τR, τ, q, c, b, t, WL, WT, W, ZL, ZT, Z, g, γ, h, νe, $\nu\mu$, $\nu\tau$, V→e, V→μ, V→τ
halo = Bur, Iso, NFW, Ein, EiB, Moo
propagation = MIN, MED, MAX
MF = MF1, MF2, MF3
mass = m_{DM} in GeV, on the range m_{DM} = 5 GeV → 100 TeV (for annihilations)

Figure 4.2: Primary channel, halo profile, propagation, magnetic field, and DM mass parameter options

The halo profile describes the distribution of dark matter density in the galaxy. The Navarro, Frenk and White profile (NFW) and the Einasto (Ein) profile are the most commonly used distributions. The NFW profile is able to describe a diverse range of halo masses, making it a useful, universal tool. The Einasto profile has emerged more recently from higher resolution simulations. The EinastoB profile (EiB) is a modification of Einasto that includes baryonic matter, producing a steeper distribution. A steep distribution also appears from the Moore profile (Moo), which is a modification of the NFW profile [29]. However, profiles fitted to simulations have a common problem of a cusp distribution, meaning the distribution shows power-law-like density behaviour, while observations indicate to the presence of a core, flat density, at the innermost parsecs of galaxies [10]. The Isothermal density profile (Iso) and the Burkert profile (Bur) fit well

with rotation curve data, as they incorporate a central core [29]. However, they are simple models that do not provide a full picture of DM halos. Since the nature of the density distribution of DM is shrouded in uncertainty, it is important to have all options available when fitting models to experimental data.

Propagation through the Milky Way Galaxy is a complicated process that is difficult to describe. Magnetic fields, gas and the aforementioned intrinsic uncertainty of DM distribution all affect calculations. The propagation parameter describes these effects governing propagation with the three options being MIN, MED, and MAX. To calculate the parameters a simplistic model is used in which the galaxy is assumed to be a disk surrounded by a magnetic field which has a cylindrical shape. DM particles annihilate in an unknown location in the galactic halo, producing positrons. The positrons travel through the magnetic field, are subjected to stellar winds, cross the galactic plane and eventually are detected at Earth. As long as the positrons stay inside the cylinder they propagate randomly and have the opportunity to be detected. If the positrons cross the edge the charged particles are no longer bound to the galaxy as the magnetic field goes to 0 outside the cylinder.

The difference between MIN, MED, and MAX is the volume of the cylinder. MAX describes the case where the cylinder is tall and the magnetic field extends to high altitudes above the galactic disk. In this condition more positrons stay within the cylinder and a higher flux of particles is detected. For MIN, which describes propagation in a minimal way, the cylinder is thin, which results in a minimal signal. MED is an intermediate case. This effect is the most important variable that distinguishes between the propagation parameters.

Figure 4.3 shows an example of a propagation flux plot with the parameters listed in the figure. The cross section that was chosen corresponds to the thermal relic DM annihilation cross section. The y-axis is by convention the energy cubed times the flux as a function of energy. And the x-axis is the positron energy.

4.2 AMS data interpretation in terms of DM

Positrons from space have been observed for a long time by cosmic ray detectors. A predicted positron signal was the flux at low energies produced by ordinary astrophysics. This signal was measured, and its source was well understood. In the late 2000s the PAMELA satellite-based cosmic ray detector orbiting Earth observed an unexpected excess of positrons at high energies [34]. This signal was later confirmed by other detectors. The source of this unforeseen measurement is still unknown and being studied. A suggestion is that the flux is produced by a local pulsar or other ordinary astrophysical phenomena. Another possibility is that the signal is a result of DM annihilations as it has been demonstrated above that such an event can produce fluxes of positrons. This is the possibility that is entertained here.

The last step of this project was to put together the positron flux predicted from DM annihilations with positron flux data measured by AMS-02. AMS-02 is an external ex-

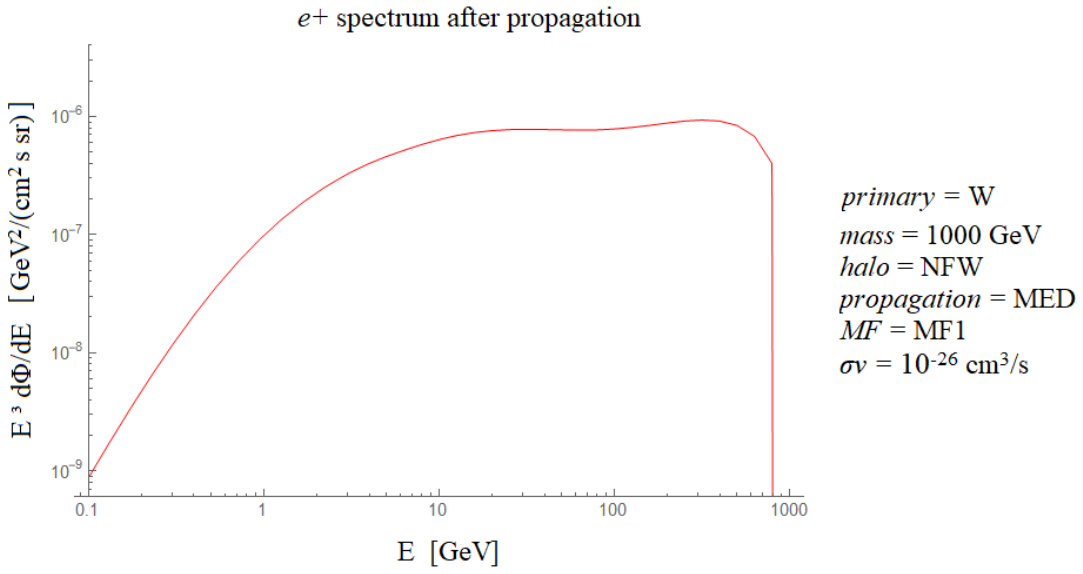

Figure 4.3: Flux of positrons at Earth after propagation from the decay of the W primary channel.

perimental module on the International Space Station which has been in operation since 2011. It is a detector designed to detect cosmic rays with a focus on antimatter. The key elements of the detector are the permanent magnet, silicone trackers, the time of flight counters (TOFs), the transition radiation detector(TRD), and the 3-dimensional sampling calorimeter (ECAL) [24]. The inclusion of the TRD makes AMS stand out as it allows the detector to distinguish between electrons and protons using transition radiation. Another advantage of the AMS detector compared to other cosmic ray detectors, such as PAMELA, is the improved electromagnetic spectrometer with 3-dimensional imaging capability which allows the measurement of high energy positrons up to 1 TeV [3]. The PAMELA detector measured positrons only up to 300 GeV [35]. As a result, AMS was able to significantly extend the measurement of the unexpected high energy positron signal.

The data was taken from the supplemental material of Ref. [36]. The article presented a measurement based on AMS positron data compiled from May 19, 2011 to November 12, 2017. The AMS data points were plotted together with the error bars, which were calculated using the uncertainties that were also provided in the supplemental material.

The energy range of the AMS data includes positrons from 0.5 GeV to 1000 GeV. The flux measured by AMS is interpreted in terms of two summed contributions: an astrophysical background, mostly concentrated at low energy and called 'diffuse term' for reasons that will be clear in a moment, and an exotic 'source term', emerging at higher energies and whose origin is unknown. The 'diffuse term' is caused by high energy cosmic rays coming in from outside the galaxy colliding with gas and dust molecules in the local galactic environment (hence the term 'diffuse') producing a variety of particles including positrons. The amount of incoming cosmic rays as well as the distribution of gas and dust has been

well studied. Therefore, physicists have been able to compute the expected diffuse term. It can be modeled with the following function [36]:

$$\Phi_{DT} = \frac{E^2}{\hat{E}^2}[C_d(\hat{E}^2/E_1)^{\gamma_d}]$$

where E is the energy of the particles, $C_d = 0.0651$ [m^2 sr s GeV]$^{-1}$ is the normalization factor, $\hat{E} = E + \phi_{e^+}$ is the energy of particles in the interstellar space with $\phi_{e^+} = 1.10$ GeV being the effective solar potential, γ_d is the spectral index, and $E_1 = 7$ GeV is a constant .

The source term, which is the positron flux that has not been predicted, is interpreted here in terms of DM and therefore is plotted using the positron flux after propagation described in Section 4.1.2. The diffuse term and source term were then summed and plotted to be able to compare theory with AMS data. In order to see which DM model fits the experimental results best, the parameters of the source term were systematically changed and the usual χ^2 test was performed. Namely, the chi-square test for goodness of fit is as follows

$$\chi^2 = \sum_{i=1}^{N_d} \left[\frac{N_i - f_i}{\sigma_i}\right]^2 \tag{4.1}$$

where N_i is the AMS measurement data points, f_i is the theoretical function of the sum of the diffuse and source term, σ_i is the standard error of each measurement, and N_d is the number data points.

As seen in Figure 4.4 the data points at low energies have very small errors, so the denominator in the χ^2 expressions for these measurements are also small. Consequently, computing χ^2 with these terms would produce a high number. The main contributor to the low energy spectrum is the diffuse term, which is not the focus of the project. In order to prevent the diffuse term to dominate χ^2, only points above 10 GeV were included. Thus, out of 74 points, only the last 49 were used. For a good fit the terms in the sum are expected to be of order 1. Hence, the goal was to find a fit which produced a χ^2 value not too far from 49.

4.2.1 Finding the best fit

The first step in finding the best fit was to choose the annihilation channel. In Figure 4.1 it has been demonstrated that most particles, such as the quarks, photons, and bosons, all produce a high flux of positrons with low energies, below 50 GeV. Therefore, they are not good candidates for the exotic high energy flux signal. On the other hand the direct annihilation channel to positrons is skewed too much to the high energy range, producing an insufficient amount of positrons in the range from 10 to 100 GeV. The two remaining viable options were the muon and tau channels.

Figure 4.4 shows the muon and tau spectra plotted with the same parameters except for an adjusted mass and cross section. Out of the two spectra, tau is the better fit; it has a χ^2 value of 203.6 while the muon spectrum has a value of 870.2 . The function is softer and has a wider range so it fills out both the intermediate and higher energy part of

the spectrum better. The reason is that the muon pairs, produced in a DM annihilation, decay immediately to electron-positron pairs creating a sharper spectrum. Taus decay to pions and muons, creating a cascade of particles with diverse range of energies, which creates a softer spectrum. Consequently, the tau spectrum was chosen as the better candidate.

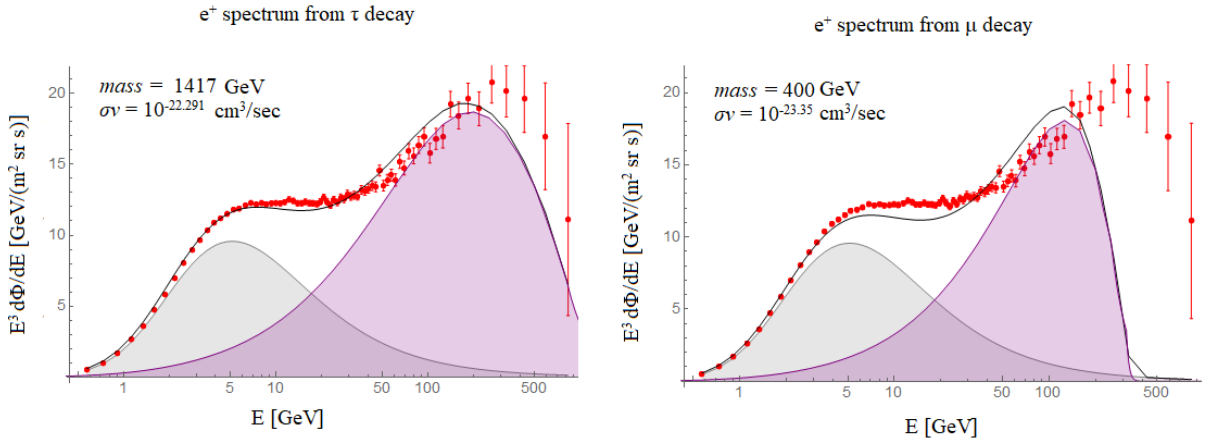

Figure 4.4: AMS data (red points) plotted with the theoretical function (black line) comprised of the diffuse term (grey area) and source term (purple area). On the left is the plot of the tau annihilation channel, on the right is the plot of the muon annihilation channel.

To better improve χ^2, the other parameters were changed. Changing the mass of DM moved the spectrum along the x-axis, since a heavier or lighter DM particle produces more energetic or less energetic positrons, respectively. Changing the annihilation cross section moved the spectrum along the y-axis, as the probability of an annihilation event directly affects the flux. All the other parameters affected the shape of the source term, and some had a significant effect on the flux as well . Figure 4.5 shows 4 plots where the parameters were systematically changed in a way to decrease χ^2. The plot with the best fit had the following characteristics: a DM mass of 1496 GeV, a cross section of $10^{-22.39}$ cm^3/sec, the EinastoB halo profile, MAX propagation, and magnetic field MF2.

4.2.2 Discussion of results

The "desired" χ^2 value was something not far from 49, and the best fit produced a χ^2 of 67.9. For a simple model where DM annihilation occurs through a single channel, this is a good result. The result could be improved by adding other annihilation particles that could account for the data points at higher energies.

In Figure 4.5 a) the initial parameters were chosen to be the Einasto density profile, medium propagation, and magnetic configuration MF1. From plot a) to b) the propagation parameter was changed to MAX, from b) to c) the magnetic configuration was changed to MF2 , and lastly from c) to d) the Einasto density profile was replaced with

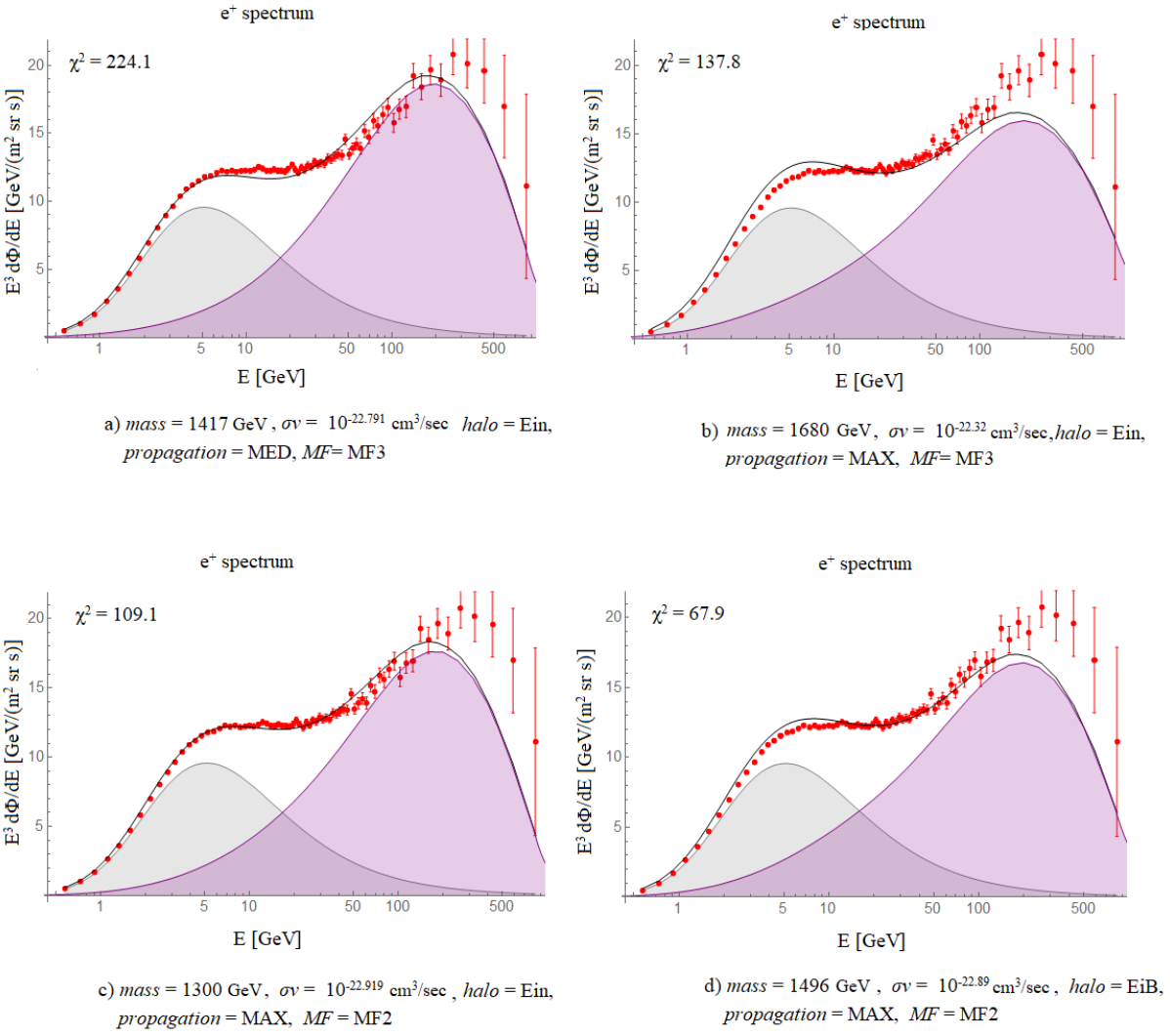

Figure 4.5: Spectrum of positrons from tau annihilation channel with changed parameters and respective χ^2 value. Plot a) shows the base plot with initial parameters, in plot b) the propagation parameter was changed, in plot c) the magnetic configuration parameter was changed, and in plot d) the density profile parameter was changed.

the EinastoB distribution. With each change the cross section and mass were adjusted to fit the function best.

It is difficult to evaluate to what extent each parameter affects the source term. For that a more extended systematic analysis has to be preformed. Nevertheless, some conclusions can still be drawn. Besides the mass and cross section, the propagation parameter seemed to have the most significant effect on χ^2 . Since the signal is produced by energetic positrons, the location of the source is likely to be nearby. The DM density distribution profiles do not differ significantly in the local region, while parameters that affect propagation can still substantially alter flux.

Due to the errors of the AMS data, plots that had the best fit to the intermediate energies were favored by χ^2. At energies above approximately 150 GeV the error bars increase significantly as a result of the high statistical error. The more positrons AMS counted in each energy bin the higher the accuracy of the measurement, and thus the lower the statistical error and error bars. Above positron energies of 150 GeV, the number of particles measured was less than 500. The number of counts further drops to below 100 for positrons with energies 500 GeV or higher. So the flux of these positrons was low and with the limited statistics the uncertainties rose. The low and intermediate energy bins had positron counts as high as 100 000, which is 4 orders of magnitude higher than the lowest flux positrons.Thus, at these energies the systematic error, which is a result of detector inaccuracy, is comparable to the statistical error, and the contributions are approximately equal. But with increasing energy, as the statistical error grew, the systematic error became subdominant.

Chapter 5

Conclusion

The thesis has reviewed the evidence for Dark Matter in the universe, the questions about its nature, and the ways to discover it. First it reviewed evidence for the existence of DM and its main properties. As DM has not yet been observed and it does not interact electromagnetically, it must be neutral. Through results from rotation curves and simulations it was shown that DM accumulates in halos, which surround galaxies like the Milky Way. These halos have the highest DM density at their center, corresponding to the innermost parsecs of the embedded galaxies. Observations also allow to conclude that DM is most likely cold and a thermal relic with a constant abundance since "freeze out".

Searches for DM are pursued through direct detection, collider experiments and indirect detection. These experiments generally rely on the weakly interacting nature of dark matter, meaning DM is assumed to only occasionally interact with SM particles and with itself. The focus of the thesis was indirect detection experiments, which search for products of DM annihilation and decay. The three main categories of indirect detection and their advantages and disadvantages were described. The first kind of experiments, gamma ray experiments, are effective as the signals are not affected by astrophysical effects and point back to the source of production. However, gamma ray backgrounds from other sources are significant and complicate the identification of DM signals. The advantage of the second kind of experiments, cosmic ray experiments, is that models of cosmic ray spectra agree well with observations, thus DM signals are easier to find. However, cosmic rays travel randomly and undergo changes during their propagation which complicates theories of cosmic ray indirect detection. An advantage of the third category, neutrino experiments, is the proximity of the DM annihilation source, as it is assumed that their is an accumulation of DM at the core of the Earth and Sun which produces a steady flux of neutrinos. However, neutrinos are difficult to detect as they interact rarely.

As part of the thesis a table of indirect detection experiments was created, containing information about their method, energy range and most recent references. The table will be featured on the future website of the initiative for Dark Matter in Europe (iDMEu) website, alongside lists of experiments for other DM detection methods. This will allow researchers as well as anyone interested in DM to be able to easily look up experiments connected to DM research on a single platform.

The thesis also included analysis of positron data from AMS-02 as potential evidence of DM. Theoretical background of positron production from DM annihilation and its propagation through the galaxy was provided. By examining the theoretical predictions it was concluded that, assuming a single annihilation channel, annihilations into tau leptons were most likely to produce the flux of positrons measured by AMS. The propagation parameters were systematically changed until the best fit was found. The analysis carried out used a simple single channel model of annihilation. A multiple channel model could have improved the results. Furthermore, a focus on the individual effects of each parameter on the positron spectra could reveal more interesting information about DM and the propagation of its charged particle annihilation products.

Acknowledgements

I would like to thank my supervisors, Marco Cirelli and Caterina Doglioni for the continuous support, patience and valuable guidance provided throughout the duration of my thesis.

References

[1] CERN. Dark matter. URL https://home.cern/science/physics/dark-matter.

[2] Bertone, G. & Hooper, D. History of dark matter. *Rev. Mod. Phys.* **90**, 045002 (2018). 1605.04909.

[3] Battiston, R. The anti matter spectrometer (AMS-02): a particle physics detector in space. *Journal of Physics: Conference Series* **116**, 012001 (2008). URL https://doi.org/10.1088/1742-6596/116/1/012001.

[4] SuperCDMS at Queen's University. Evidence for dark matter. URL https://cdms.phy.queensu.ca/Public_Docs/DM_Intro.html.

[5] Cornel University, Department of Astrophysics. Rotation curves. URL http://hosting.astro.cornell.edu/academics/courses/astro201/rotation_curves.htm.

[6] Zasov, A. V., Saburova, A. S., Khoperskov, A. V. & Khoperskov, S. A. Dark matter in galaxies. *Physics-Uspekhi* **60**, 3–39 (2017). URL http://dx.doi.org/10.3367/UFNe.2016.03.037751.

[7] NASA's Chandra X-ray Observatory and John F. Kennedy Space Center. Plain, C. A matter of fact. URL https://www.nasa.gov/vision/universe/starsgalaxies/dark_matter_proven.html.

[8] Encyclopaedia Britannica (2017). Gravitational lens. URL https://www.britannica.com/science/gravitational-lens.

[9] NASA. Nemiroff, R. & Bonnell, J. Astronomy picture of the day (2006). URL https://apod.nasa.gov/apod/ap060824.html.

[10] Lisanti, M. Lectures on dark matter physics. *New Frontiers in Fields and Strings* (2016). URL http://dx.doi.org/10.1142/9789813149441_0007.

[11] NASA/IPAC Extragalactic Database. Kolb, E. Particle physics in the early universe: Inflation. URL https://ned.ipac.caltech.edu/level5/Kolb/Kolb3.html.

[12] Sun.org - Your Online Museum of the Universe. A short history of the universe (2020). URL http://www.sun.org/encyclopedia/a-short-history-of-the-universe.

[13] OSU Astronomy. Weinberg, D. Introduction to cosmology: Dark matter and structure formation. URL http://www.astronomy.ohio-state.edu/~dhw/A5682/index.html.

[14] Hu, W. & White, M. The cosmic symphony. *Scientific American* **290**, 44–53 (2004).

[15] Peter, A. H. G. Dark matter: A brief review (2012). 1201.3942.

[16] ParticleBites - The high energy physics reader's digest. Green, A. Dark matter freeze out: An origin story (2020). URL https://www.particlebites.com/?p=7004.

[17] NASA/IPAC Extragalactic Database. Kolb, E. Particle physics in the early universe: Dark matter. URL https://ned.ipac.caltech.edu/level5/Kolb/Kolb5_1.html.

[18] CERN. Lopes, A. Breaking new ground in the search for dark matter (2020). URL https://home.cern/news/series/lhc-physics-ten/breaking-new-ground-search-dark-matter.

[19] Profumo, S. Tasi 2012 lectures on astrophysical probes of dark matter (2013). 1301.0952.

[20] Hooper, D. Tasi lectures on indirect searches for dark matter (2018). 1812.02029.

[21] Fermi Gamma Ray Space Telescope. Fermi searches for dark matter (2016). URL https://fermi.gsfc.nasa.gov/science/eteu/dm/.

[22] Cherenkov Telescope Array Observatory. Detecting cherenkov light. URL https://www.cta-observatory.org/about/how-cta-works/.

[23] HAWC: the High-Altitude Water Cherenkov Gamma-Ray Observatory. Detecting cosmic rays. URL https://www.hawc-observatory.org/science/detection.php#sec:iact_eas.

[24] The Alpha Magnetic Spectrometer on the International Space Station. Ams-02 detector. URL https://ams02.space/detector.

[25] DArk Matter Particle Explorer. Dampe. URL http://dpnc.unige.ch/dampe/.

[26] Fukuda, Y. *et al.* The Super-Kamiokande detector. *Nucl. Instrum. Meth. A* **501**, 418–462 (2003).

[27] Halzen, F. & Klein, S. R. Invited review article: Icecube: An instrument for neutrino astronomy. *Review of Scientific Instruments* **81**, 081101 (2010). URL http://dx.doi.org/10.1063/1.3480478.

[28] Inc., W. R. Mathematica, Version 11.3. Champaign, IL, 2018.

[29] Cirelli, M. *et al.* PPPC 4 DM ID: a poor particle physicist cookbook for dark matter indirect detection. *Journal of Cosmology and Astroparticle Physics* **2011**, 051–051 (2011). URL http://dx.doi.org/10.1088/1475-7516/2011/03/051.

[30] Ciafaloni, P. *et al.* Weak corrections are relevant for dark matter indirect detection. *Journal of Cosmology and Astroparticle Physics* **2011**, 019–019 (2011). URL http://dx.doi.org/10.1088/1475-7516/2011/03/019.

[31] Sjöstrand, T., Mrenna, S. & Skands, P. A brief introduction to PYTHIA 8.1. *Computer Physics Communications* **178**, 852–867 (2008). URL http://dx.doi.org/10.1016/j.cpc.2008.01.036.

[32] Beringer, J. *et al.* Review of particle physics. *Phys. Rev. D* **86**, 010001 (2012). URL https://link.aps.org/doi/10.1103/PhysRevD.86.010001.

[33] Buch, J., Cirelli, M., Giesen, G. & Taoso, M. PPPC 4 DM secondary: a poor particle physicist cookbook for secondary radiation from dark matter. *Journal of Cosmology and Astroparticle Physics* **2015**, 037–037 (2015). URL http://dx.doi.org/10.1088/1475-7516/2015/09/037.

[34] Cholis, I., Finkbeiner, D. P., Goodenough, L. & Weiner, N. The PAMELA positron excess from annihilations into a light boson. *Journal of Cosmology and Astroparticle Physics* **2009**, 007–007 (2009). URL http://dx.doi.org/10.1088/1475-7516/2009/12/007.

[35] Picozza, P. *et al.* PAMELA – a payload for antimatter matter exploration and light-nuclei astrophysics. *Astroparticle Physics* **27**, 296–315 (2007). URL http://dx.doi.org/10.1016/j.astropartphys.2006.12.002.

[36] Aguilar, M. *et al.* Towards Understanding the Origin of Cosmic-Ray Positrons. *Phys. Rev. Lett.* **122**, 041102 (2019).